



**Atmospheric Density Variations at 1500-4000 km
Height Determined from Long Term Orbit
Perturbation Analysis**

Bruce R. Bowman

**Space Warfare Center, AE
Astrodynamics Branch**

SCHRIEVER AFB CO 80912

**AAS/AIAA Space Flight
Mechanics Meeting**

Santa Barbara, California

11-14 February 2001

AAS Publications Office, P.O. Box 28130, San Diego, CA 92198

Atmospheric Density Variations at 1500-4000 km Height Determined from Long Term Orbit Perturbation Analysis

Bruce R. Bowman*

Atmospheric density values have been determined from analysis of the orbit perturbations of 25 satellites in the height range of 1500 km to 4000 km. The selected satellites were 18 West Ford needle clusters, 5 Delta rocket body debris pieces, and 2 balloon satellites (Dash-2 and Pageos). Over 30 years of NORAD semi-major axis values, at 5 to 10-day intervals, were used for most satellites of this analysis. All of the satellites have large area-to-mass (A/M) ratios enabling good long-term observability of the semi-major axis variations, even at these low drag exospheric heights. Using the long term solar radiation pressure A/M fitted values allowed 1 to 2-year average density factors to be computed, with almost 500 average density factors obtained over a time span of three 11-year solar cycles. The density values were computed as correction factors of the CIRA72 (Jacchia 1971) model atmosphere, and were fitted as a function of height and $\bar{F}_{10.7}$ values. The density variations were also compared with the MSISE-90 atmospheric model. The density values obtained from the orbital data were 100% to over 300% greater than either model predicted, depending upon height and $\bar{F}_{10.7}$. Density values obtain from Smithsonian Astrophysical Observatory (SAO) analysis of the Dash-2 balloon orbital decay were found to be in excellent agreement with the analysis results. Average atmospheric temperature values when helium was dominant were computed from the density values using the CIRA72 atmosphere temperature profiles. The average temperature values were found to be in excellent agreement with the few temperature values computed by SAO for the Dash-2 decay. The variation in the temperature with respect to $\bar{F}_{10.7}$ was found to increase significantly with increasing altitude between 1500 km and 4000 km. This is in contrast with the CIRA72 model that maintains a constant ratio of temperature increase with respect to $\bar{F}_{10.7}$ independent of height.

INTRODUCTION

All atmospheric models developed to date have only incorporated neutral density values below 1000 km due to lack of data at the higher altitudes. The models developed by Jacchia (1970,1971,1977) only used a few satellites to correlate long term density variations with the 11-year variation of $\bar{F}_{10.7}$ index, and those satellites were all below 800 km altitude. Later work by Hedin (1983,1987,1991) in developing the MSIS models still used only density data below 1000 km. Only a handful of density analyses have been done for

* Astrodynamics Branch, Space Warfare Center AE, Schriever AFB CO 80912

satellites in the 1500 km to 4000 km height range. A number of papers were published in the 1970s based on analyses of the orbital decay of the Pageos 1 and Dash-2 balloons. Dash-2, launched in 1963, was a 3-meter diameter balloon that decayed in 1971. Pageos 1, launched in 1966, was a 30-meter balloon that broke up several times from 1975 to 1986, and the largest piece is still in orbit today. Fea (1970) determined an upper limit for density at 3500 km from his analysis of 1964 Dash-2 data. Prior (1971) found hydrogen concentrations about 3 times that of the U.S. Standard 1966 Atmosphere Supplement for both Pageos and Dash-2 during 1967 when they were at approximately 3500-km altitude. Rousseau (1973) analysed Dash-2 data in the height range of 1500 to 3000 km and found that the Jacchia 1970 model underestimated the density values by about a factor of 3. Slowey (1974) reduced Dash-2 data for selected time spans between 1964 and 1971, and found the Jacchia 1970 model again underestimated the density by about a factor of 3.

All the above analyses for the height range of 1500 km to 4000 km covered only a short time span relative to the solar 11-year sunspot cycle, and thus no correlation was obtained between density variations and the 11-year variation in $\bar{F}_{10.7}$ solar index. For heights below 1500 km, Pardini (1999) analyzed the drag of the Japanese AJISAI satellite, and found that the 1990 MSISE atmospheric model (MSIS90) underestimated the computed density values by 30% to 50% during low solar activity. For heights greater than 4000 km, only the Lageos satellite orbit at 5900 km has yielded any density data. Rubican (1990) and Afonso (1985) analyzed the drag accelerations due to charged and neutral particle drag. However, no correlation has yet been obtained above 1000 km for the density variations as a function $\bar{F}_{10.7}$. It is the purpose of this paper to present the analysis of over 30 years of density data in the height range of 1500 km to 4000 km obtained from 25 satellite orbits, and to formulate density variations with respect to altitude and the $\bar{F}_{10.7}$ index.

ANALYSIS METHOD

The analysis method was reported previously (Bowman, 1999) from the long-term orbit perturbation analysis of West Ford needles' orbits. A semi-analytical integrator (Bowman, 1999) was developed using the perturbations in the semi-major axis for atmospheric drag, solar radiation pressure, and earth albedo. The drag equations consisted of orbit-averaged perturbation equations derived by King-Hele (1964). The drag equations are based on an atmospheric density value obtained at approximately $\frac{1}{2}$ scale height above the perigee point. With this method King-Hele has shown that an error of up to 25% in scale height results in an error of only 1.5% or less in the drag perturbation. The solar radiation pressure equations employed were orbit-averaged equations in the semi-major axis developed by Koskela (1962). The earth albedo model consisted of orbit averaged equations developed by Anselmo (1983), where albedo perturbations on the semi-major axis accounted for the albedo differences of the northern and southern hemispheres, and the strong seasonal albedo dependencies that have been observed.

The atmospheric drag equations required modification for the variation of the drag coefficient. For a circular satellite below 600 km height, the C_D value remains almost constant at 2.2. As the height increases, the lighter molecular species start becoming predominant, depending upon the level of solar activity present. At 3500 km the C_D value can be higher than 4.0, where hydrogen is the dominant species. The drag coefficient depends upon the reflectivity of the satellite as well as the relative velocity of the satellite with respect to the surrounding medium. When the velocity of the satellite, V_s , is greater than the thermal velocity of the gas particles, V_T , the drag coefficient can be expressed (Afonso, 1985) as

$$C_D = \delta \left[2 + \frac{4}{3} \left(\frac{V_T}{V_s} \right)^2 - \frac{2}{15} \left(\frac{V_T}{V_s} \right)^4 \right] \quad (1)$$

where δ is the accommodation coefficient representing the reflective properties of the satellite's surface. For a perfect absorber $\delta=1$, and for $\delta=2$ all the incoming particles are reemitted in the opposite direction to the satellite motion. For a spherical aluminum satellite Alfonso gives the following tables for δ and C_D , assuming a diffuse reemission process and a hyperthermal free flow (satellite velocity greater than thermal velocity).

Accommodation Coef δ	
Hydrogen	1.4
Helium	1.3
Oxygen	1.1

Table 1. Accommodation coefficient δ for different molecular species.

T(K)	Hydrogen		Helium		Oxygen	
	V_T/V_S	C_D	V_T/V_S	C_D	V_T/V_S	C_D
800	0.72	3.71	0.36	2.82	0.18	2.25
1200	0.88	4.14	0.44	2.93	0.22	2.27
2000	1.14	4.90	0.57	3.15	0.29	2.32

Table 2. Drag coefficient C_D and relative thermal velocity V_T/V_S as a function of atmospheric temperature and molecular species.

From the tables it is easy to see that the C_D value can increase from both an increase in δ and an increase in the V_T/V_S ratio due to lighter molecular species becoming the dominant density constituents. From 1500 km to 4000 km the dominant species changes from helium to hydrogen, depending upon the level of solar activity present.

The next step in the analysis was to develop a non-linear least squares program to fit the NORAD mean semi-major axis (a) values. For each satellite included in the analysis the semi-major axis was integrated over a data span between 20 and 35 years, depending upon data availability. The perturbations from the orbit-averaged equations were integrated over the span with a 2-day step size. The semi-major axis was used as the element of interest, since there are no long periodic or secular perturbations in a from any gravitational effects for these orbits of interest. NORAD mean elements were available every 3 to 10 days for the satellites for up to 35-year time spans. During the integration the other predicted orbital elements were constrained to the values of the real mean elements obtained from the NORAD element sets. This method avoids non-linear variations in a , and allows good convergence in the solution coefficients. The long term solution parameters included density correction factors for hydrogen and helium, a direct solar radiation pressure coefficient, the initial semi-major axis value, and several long term albedo coefficients (Bowman, 1999). The drag coefficient C_D was modeled as previously discussed. Each fit consisted of using 500 to 1000 sets of orbit elements. The density factors obtained for hydrogen and helium represent 20 to 35-year averages of density variations at altitudes above 1500 km. The density factors are multiplication factors of the CIRA72 species densities before all the species densities are combined into the model density value used in the drag equations. The CIRA72 model atmosphere was selected for the analysis because it integrates the diffusion equations to any altitude as opposed to using predefined lookup tables that stop at 2500-km altitude. The previous paper (Bowman, 1999) lists the fit results for 20 West Ford needles clusters. Figure 1 shows the perturbations for one of the needles clusters, satellite 02377, which remained at approximately 3500-km altitude for the 35-year fit span. The graphed perturbations were computed using the fitted solution coefficients. Figure 2 shows the resulting residuals from the best fit solution for this satellite.

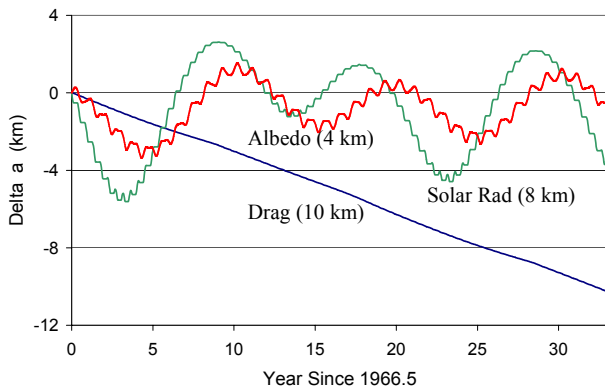


Fig. 1 Perturbations of the semi-major axis of satellite 02377

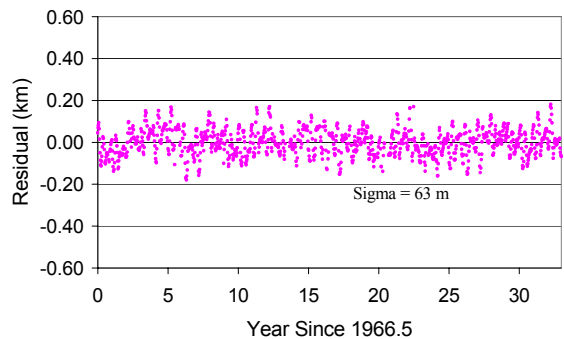


Fig. 2 Residuals in semi-major axis for satellite 02377 fit.

The long-term (20 to 35 year) best fit solution for each satellite contains the solar radiation pressure and albedo coefficients for the satellite. The previous analysis (Bowman, 1999) demonstrated that the satellite area-to-mass (A/M) ratio could be determined within 15% accuracy using each satellite solution's long-term solar radiation pressure coefficient. Once the A/M ratio was determined, short-term density factors could be obtained by holding the long-term solar radiation pressure and albedo coefficients constant, and fitting only the initial a and one density factor for each short interval selected. The density factor represents a 1 to 2-year average compared with the CIRA72 density values. Fits of less than 1 year showed too much variability in the drag coefficients, which is typical of least squares orbit determinations when coefficient observability is a problem. Thus, the short term fit spans were limited to 1 to 2-year intervals based on drag coefficient observability.

ANALYSIS SATELLITES

Density factors were obtained for 25 satellites spanning a period of over 30 years. Table 3 lists the satellites that were used for the analysis. Eighteen West Ford Needles clusters were used in the height range of 1450 km to 3600 km. All the needles clusters had large A/M ratios greater than 0.75. Five pieces of Delta 1 rocket body debris were used for density variations in the height range of 1600 to 1750 km. The A/M ratios of these pieces were all greater than 0.10, which was sufficient to determine density variations at these lower altitudes.

NORAD	Satellite	Height Range (km)	A/M Value
624	Dash-2 Balloon	1500-2400	4.04
2253	Pageos Balloon	2200-3600	9.27
2359	Needles cluster	2800-3600	1.52
2360	Needles cluster	1650-3600	2.06
2362	Needles cluster	2200-3600	1.32
2363	Needles cluster	1450-3600	1.63
2364	Needles cluster	3400-3600	0.75
2367	Needles cluster	1650-2800	1.57
2374	Needles cluster	1550-3500	1.70
2375	Needles cluster	2200-3600	1.19
2377	Needles cluster	3100-3600	0.97
2379	Needles cluster	2400-3600	1.28
2380	Needles cluster	3000-3600	1.17
2496	Needles cluster	1450-3600	1.84
2530	Needles cluster	3000-3600	1.20
2796	Needles cluster	2900-3600	1.02
3235	Needles cluster	1800-2800	1.89
3257	Needles cluster	3400-3600	0.98
10837	Delta 1 debris	1600-1650	0.12
12647	Delta 1 debris	1650-1750	0.56
13529	Delta 1 debris	1700-1750	0.15
13533	Delta 1 debris	1650-1700	0.19
13539	Delta 1 debris	1650-1700	0.13
18962	Needles cluster	1450-1850	1.53
19002	Needles cluster	1600-3600	2.00

Table 3. Satellites used for the 1500 km to 4000 km altitude analysis.

Finally, two balloon satellites, Pageos-1 and Dash-2, were used. The Dash-2 was a 3-meter diameter balloon launched in 1963 with the West Ford needles. It decayed in 1971 after solar radiation pressure forced the perigee height down from its near circular 3600-km initial orbit. This balloon was tracked extensively by USAF and Smithsonian Astrophysical Observatory (SAO) Baker-Nunn cameras, and high precision ephemerides were obtained by SAO (Slowey, 1974). The Dash-2 data included in this analysis covered a height range of 1500 km to 2400 km. Also used in this evaluation were Slowey's density and temperature data obtained from drag analysis during periods when the orbit was entirely sunlit with no shadow crossings occurring. Slowey found that unexpected solar radiation perturbations occurred during periods when the orbit was eclipsed by the earth's shadow. The non-eclipse density values obtained by Slowey were compared to the CIRA72 model, and density factors were computed for the data. The factors were averaged over one solar rotation period (approximately 27 days) and are plotted on the data graphs.

The second balloon satellite used in this analysis was Pageos-1, a 30-meter diameter balloon launched in 1966 for geodetic studies. This balloon was tracked extensively by USAF and SAO Baker-Nunn cameras until the early 1970s. The balloon broke up several times from 1975 to 1985. Following the last breakup in 1985 the largest piece still left in orbit had an A/M value of 9.0, which appeared to be stable over the last 15 years. During this period the perigee height changed from 3600 km to 2200 km, and this is the data that was included in the analysis.

DENSITY FACTOR COMPUTATIONS

Following determination of the 1 to 2-year average density factors for each satellite, the data was plotted with respect to time and the 81-day average $\bar{F}_{10.7}$ solar index. Figure 3 shows an example of the data obtained for the needle cluster 02530 over the 30-year period of analysis for this satellite. The factors can be separated into periods when hydrogen was dominant ($\rho_{\text{He}}/\rho_{\text{H}} < 0.3$), when helium was dominant ($\rho_{\text{He}}/\rho_{\text{H}} > 3$), and when an approximately even mixture of hydrogen and helium occurred. The CIRA72 model was used to determine the concentration of each species. Satellite 02530 remained in the height range of 3000 km to 3600 km during the entire 30-year span. Figure 3 shows that hydrogen was dominant during periods of low solar activity ($\bar{F}_{10.7} < 90$), while helium was dominant during periods of high solar activity ($\bar{F}_{10.7} > 150$). Figure 4 shows the same data plotted as a function of $\bar{F}_{10.7}$. The scatter in the data is a result of the averaging of the density over the 2-year fit spans used for this satellite. During any 2-year span the average perigee height varied by about 230 km, while the $\bar{F}_{10.7}$ value varied by about 50.

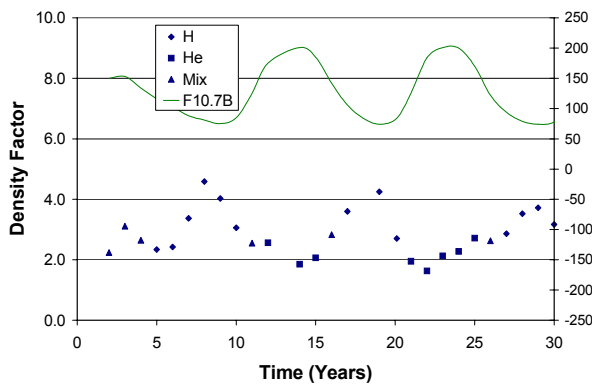


Fig. 3 Sat 02530 density factors vs time.

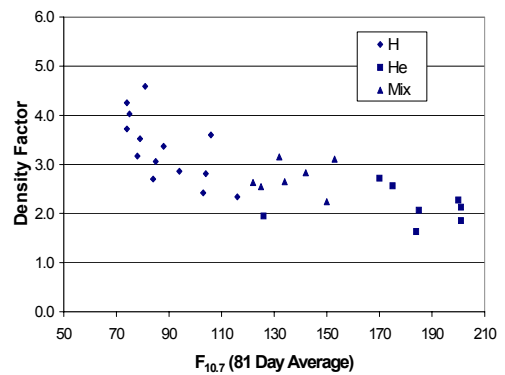


Fig. 4 Sat 02530 density factors vs $\bar{F}_{10.7}$

Approximately 500 density factors were obtained from data from all 25 satellites covering more than 30 years of time. Figure 5 shows the sample of data obtained for the height range of 1500 km to 2000 km. Thirteen satellites were available for use in this height range, and the values of $\bar{F}_{10.7}$ spanned the entire region of low to high solar activity covering three 11-year solar cycles. The needles clusters are displayed as triangles, the Delta debris as boxes, and the Dash-2 satellite 00624 is displayed with x symbols.

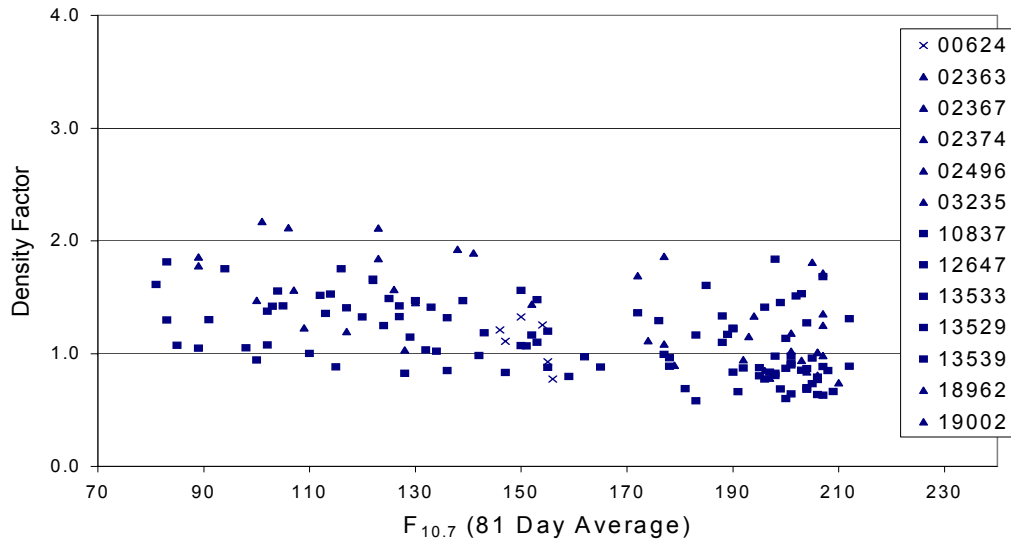


Fig. 5. Density factors for 1500-2000 km altitude vs. $\bar{F}_{10.7}$.

The density factors were then fit as a function of height and $\bar{F}_{10.7}$. The resulting equation (Equation 2) is plotted as the New Model parameter in the different altitude graphs. Figures 6 through 14 show the density factors and the New Model fit for each height range as a function of $\bar{F}_{10.7}$. For comparison purposes the 1990 MSISE atmospheric model (MSIS90) values are also plotted for each altitude range. The factors for the MSIS90 model were obtained by averaging over all latitudes and longitudes throughout an entire year for a given height and $\bar{F}_{10.7}$ value ($F_{10.7}$ was set to $\bar{F}_{10.7}$), and compared to the CIRA72 averaged value. The averaging over geography and time removed any variation in the density due to the diurnal and semi-annual density variations, and should correspond to the 1 to 2-year average density factors obtained for the satellites.

Figure 6 shows the data used in the height range of 1450 km to 1700 km. The New Model fit and MSIS90 results are plotted for the 1500-km height. The MSIS90 model is close to the CIRA72 model (density factor = 1.0) but fits the data better for medium to high solar activity. Figure 7 shows the data for the 1700 km to 1800 km height. Again, the MSIS90 models the slope more closely for medium to high solar activity. Pardini (1999) found from analyzing the drag on the AJISAI satellite that during low solar activity MSIS90 underestimated the real density by 30% to 50% at 1500-km altitude. This is in excellent agreement with the Figure 6 results. Figure 6 also shows 3 plotted values of the SAO density values obtained from the Dash-2 analysis. The error bars represent the deviation over one solar rotation cycle (approximately 27 days) of the SAO density values obtained late in the life of the satellite. The satellite's perigee height only remained for a year within this height band of 1700 km to 1800 km. The SAO data fits the New Model much better than the CIRA72 or MSIS90 models.

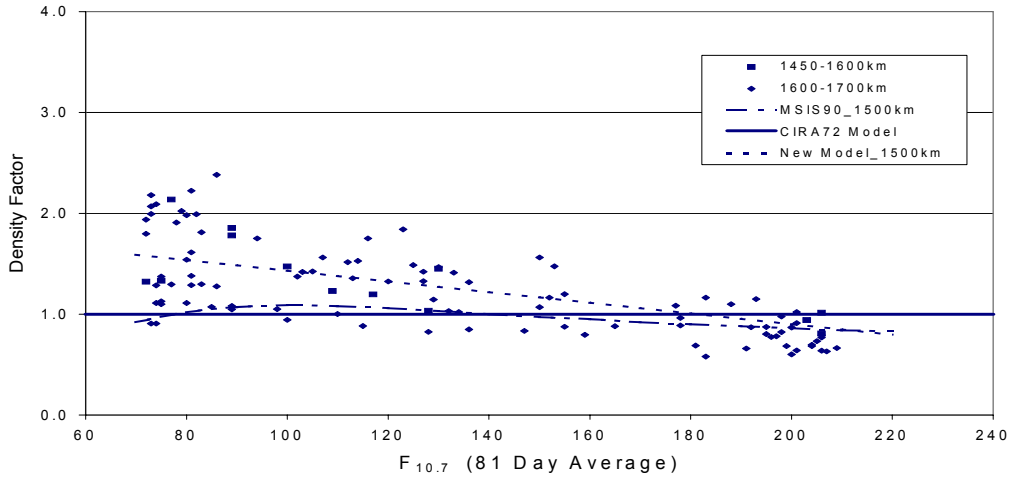


Fig. 6 Density factors for the 1450-1600 km altitude region.

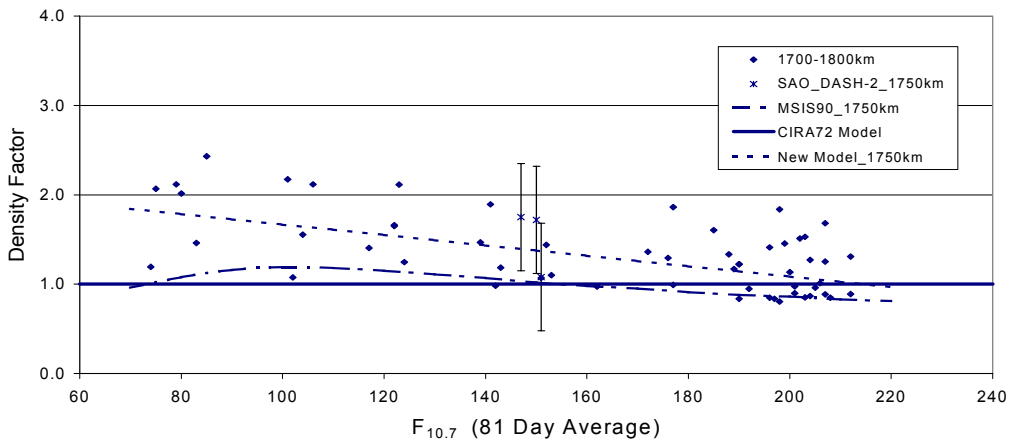


Fig. 7 Density factors for the 1700-1800 km altitude region.

Figures 8 through 12 show a progression of data from 1800 km to 3000 km altitude. The New Model fit shows a widening variation occurring between the real data and the CIRA72 or MSIS90 models. The MSIS90 model's slope still fits the data better for medium to high solar activity. However, for lower solar activity, the MSIS90 model deviates more as the altitude increases. Figures 13 and 14 show the models for the height regions above 3000 km. Dash-2 SAO data was also available for these heights and is plotted with error bars in Figure 13. Again, the SAO data agrees very well with the New Model fit. The scatter in the data is greater above 3000 km than below due to the observability problem of measuring drag effects at heights where the atmospheric density is very small.

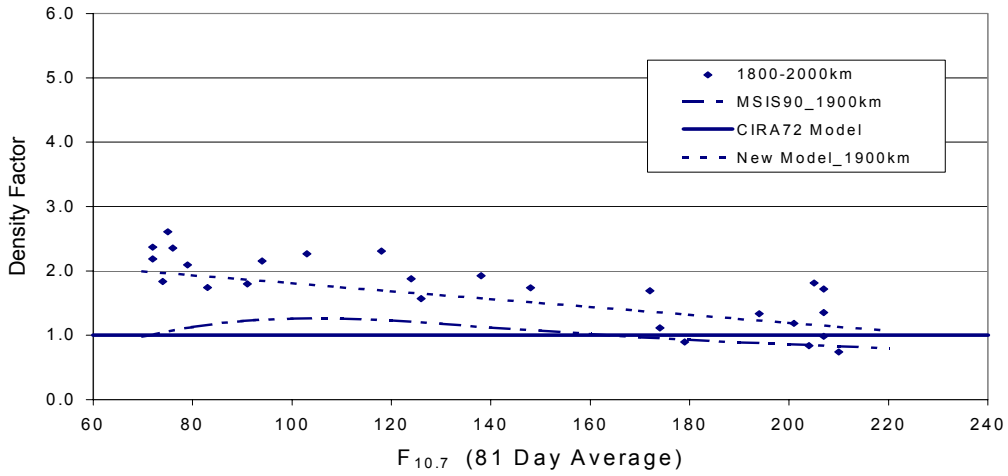


Fig. 8 Density factors for the 1800-2000 km altitude region.

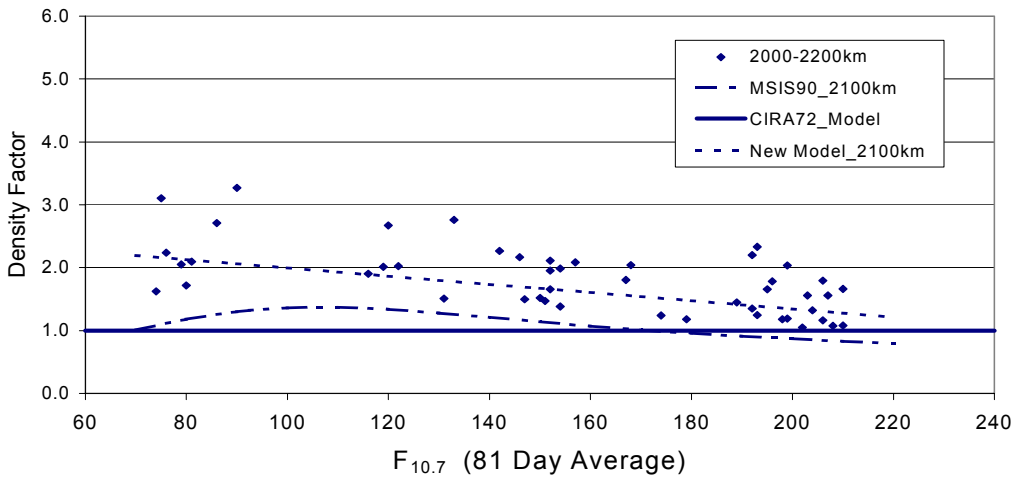


Fig. 9 Density factors for the 2000-2200 km altitude region.

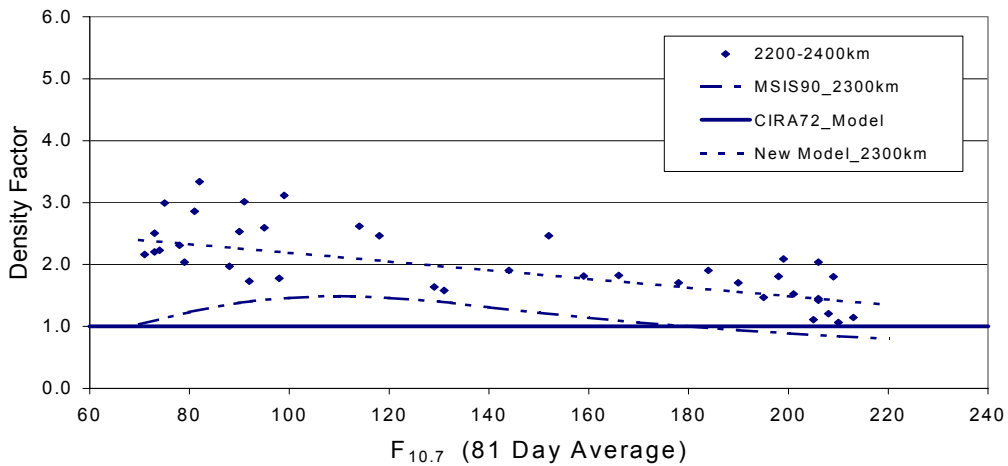


Fig. 10 Density factors for the 2200-2400 km altitude region.

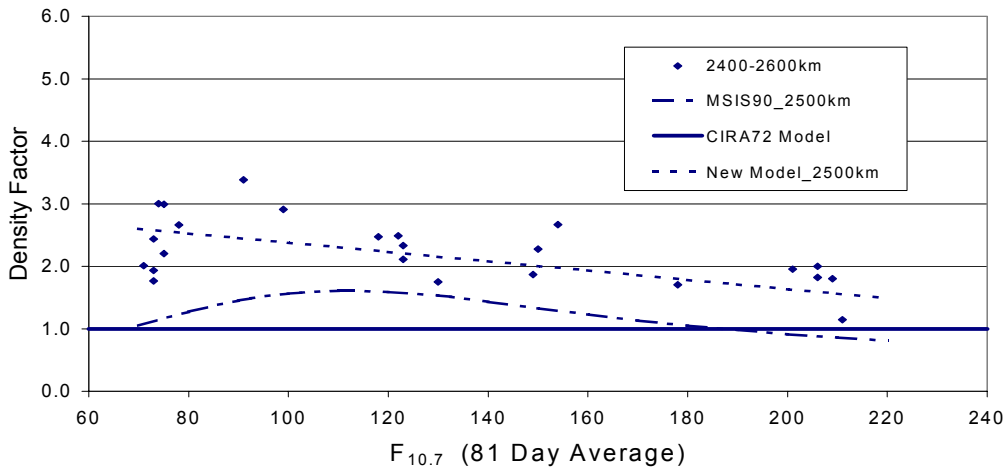


Fig. 11 Density factors for the 2400-2600 km altitude region.

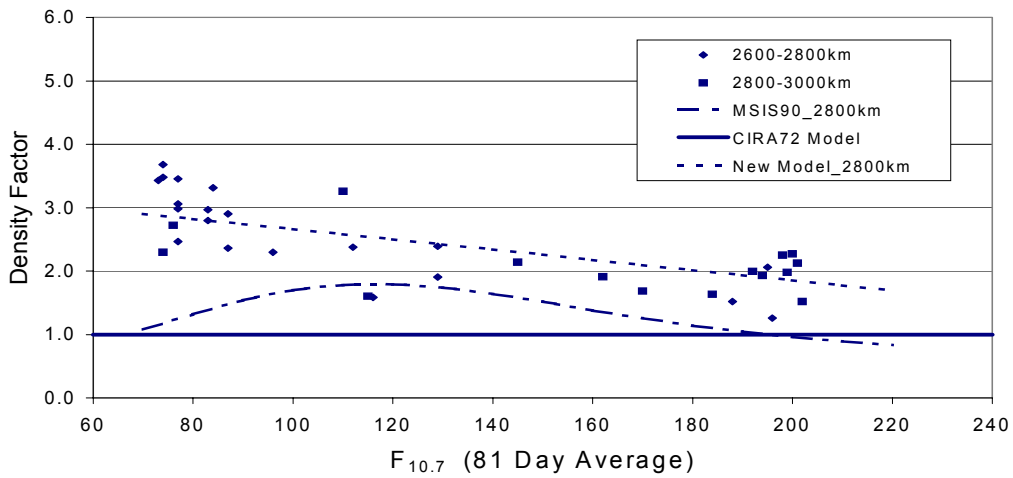


Fig. 12 Density factors for the 2600-3000 km altitude region.

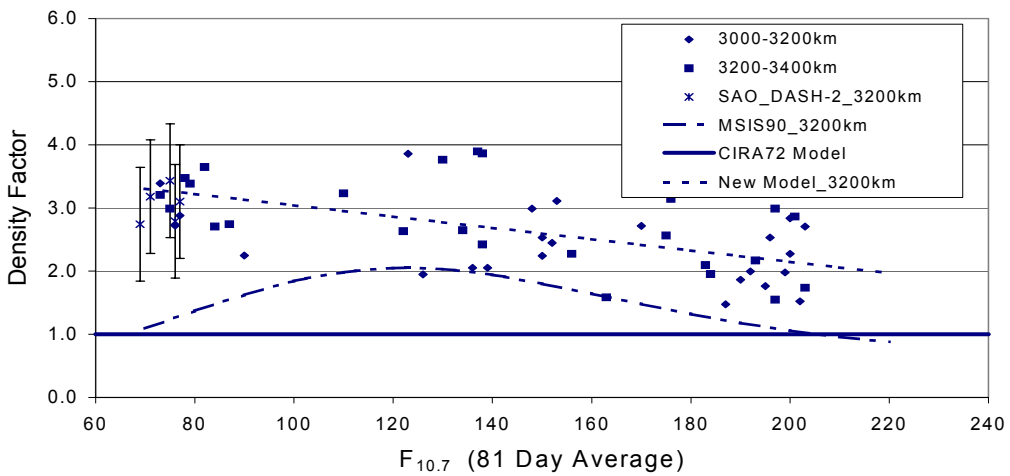


Fig. 13 Density factors for the 3000-3400 km altitude region.

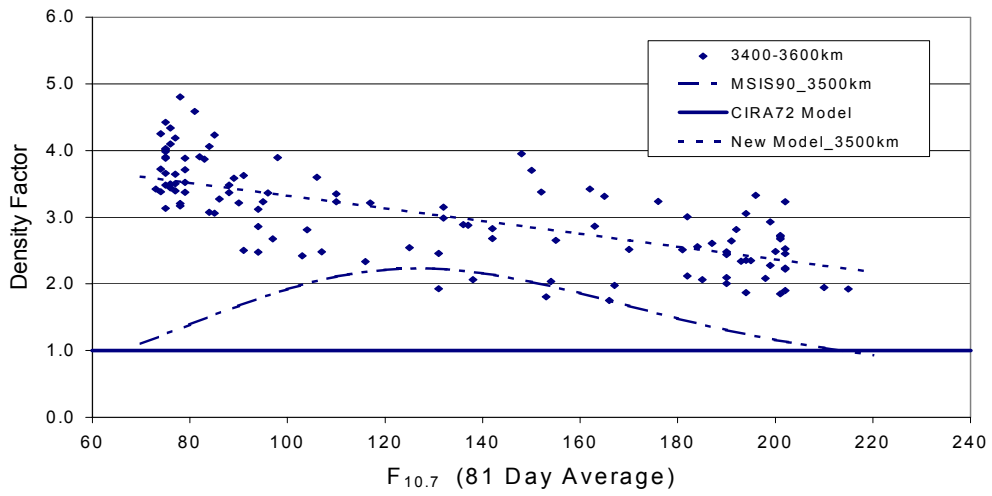


Fig. 14 Density factors for the 3400-3600 km altitude region.

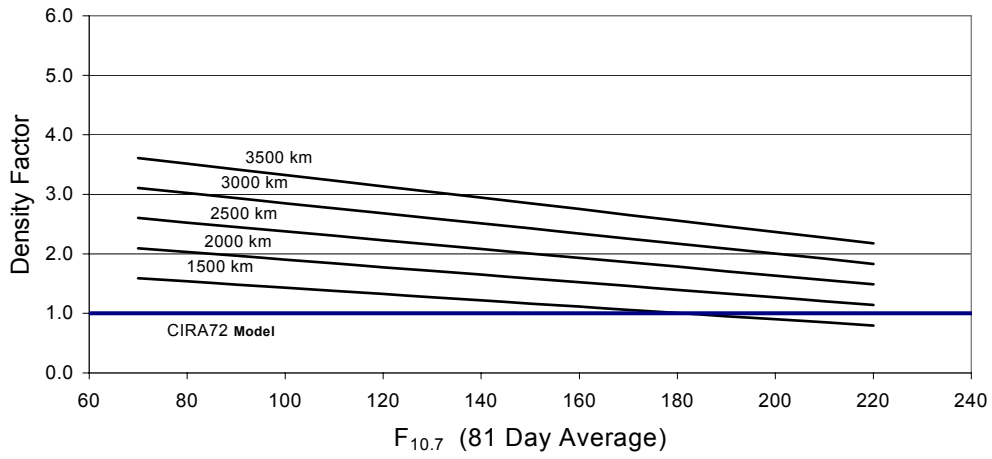


Fig. 15 Density factors from the New Model least squares fit.

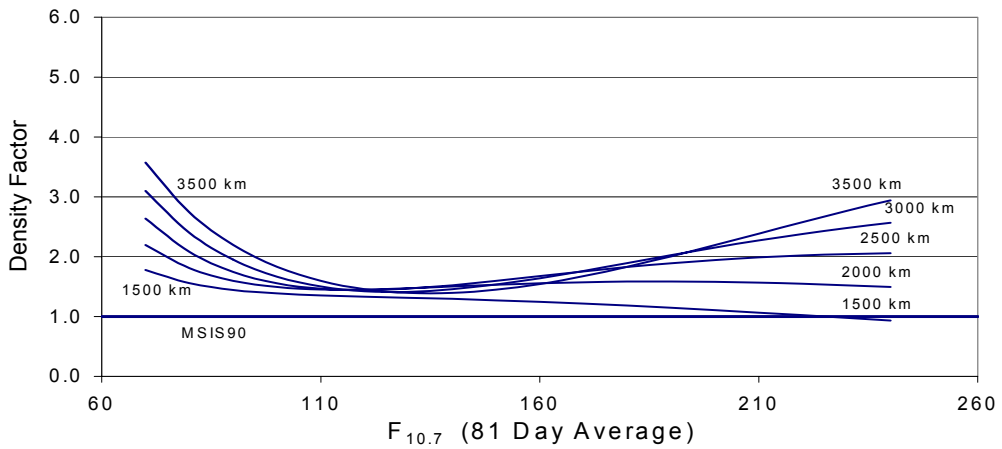


Fig. 16 New Model density factors for MSIS90 atmospheric model.

The New Model fit is shown in Figure 15 as a function of height and $\bar{F}_{10.7}$ values. The least-squares model obtained from fitting the factor data is

$$F_{\rho} = C_0 + C_1 \bar{F}_{10.7} + C_2 H + C_3 H \bar{F}_{10.7} \quad (2)$$

where

$$H = \text{Height (km)}, \quad \bar{F}_{10.7} = 81\text{-day } F_{10.7} \text{ average}$$

$$C_0 = 0.22 \pm 0.19$$

$$C_1 = -0.200\text{E-}02 \pm 0.13\text{E-}02$$

$$C_2 = 0.115\text{E-}02 \pm 0.73\text{E-}04$$

$$C_3 = -0.211\text{E-}05 \pm 0.51\text{E-}06$$

F_{ρ} is the density factor to apply to the CIRA72 model density. The standard deviation σ_F of the density factors is 0.42, while the standard deviation for the New Model fitted function is 0.05.

Figure 16 shows the New Model factors in comparison with the MSIS90 model ($F_{\rho} = 1.00$). The low solar activity values deviate much more rapidly than for high solar activity, while $\bar{F}_{10.7} = 120$ appears to fit the New Model parameters with a factor of 1.5 for all heights. This means that the MSIS90 model is really underestimating the hydrogen concentration at low solar activity, and also underestimating the helium density at high solar activity, although not as much as for the hydrogen estimation.

TEMPERATURE ANALYSIS

An average global night-time minimum temperature value was computed for each 1 to 2-year fitted span using the temperature profiles from the CIRA72 model. This was accomplished by computing the temperature from CIRA72 every 2 days during the time span, and applying the least squares fitted density factor at each integration step. The temperatures were then compared to the CIRA72 temperatures without the density factor applied, and temperature correction factors were obtained. The corrected nighttime exospheric temperature factor and $\bar{F}_{10.7}$ were then selected at the midpoint of the data span.

The temperature data was first analyzed for time periods when Helium (He) was dominant. Figure 17 shows the He temperature values obtained for the 1450 km to 1700 km height range. A linear fit is also displayed on the graph. In another example, Figure 18 shows the He temperatures for the 1700 km to 2000 km range. Several temperature points were also available during this time from the SAO analysis of the Dash-2 data. The error bars are a result of averaging the daily temperatures over one 27-day solar rotation period. The SAO temperature values are in good agreement with the temperature data obtained from the fitted density factor data. As a final example, Figure 19 shows the He temperature data for the 3200 km to 3600 km high end altitude range. The He temperatures are for mid to high solar activity ($\bar{F}_{10.7} > 140$) at these altitudes because hydrogen is dominant during low solar activity for heights above 3000 km. The resulting slopes of temperature vs $\bar{F}_{10.7}$ when He was dominant are shown in Figure 20. The CIRA72 slope is also plotted as a constant value, which Jacchia (1970) determined from several satellites at altitudes below 800 km. The new temperature slopes show a definite decrease with decreasing altitude, indicating that there is less response to solar activity for He as the altitude decreases. There was not enough data for the same analysis when hydrogen was dominant, but the few temperature slopes that could be obtained indicated that the same pattern was present for hydrogen.

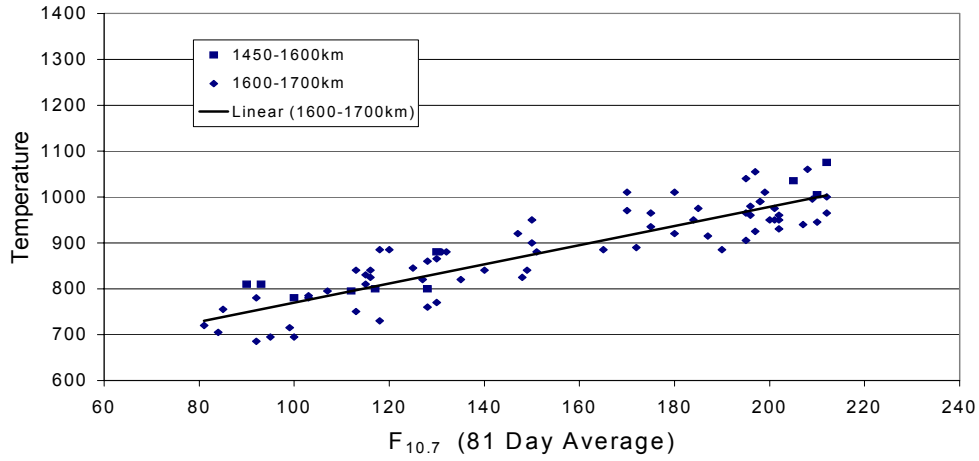


Fig. 17 He temperature for the 1450-1700 km altitude region.

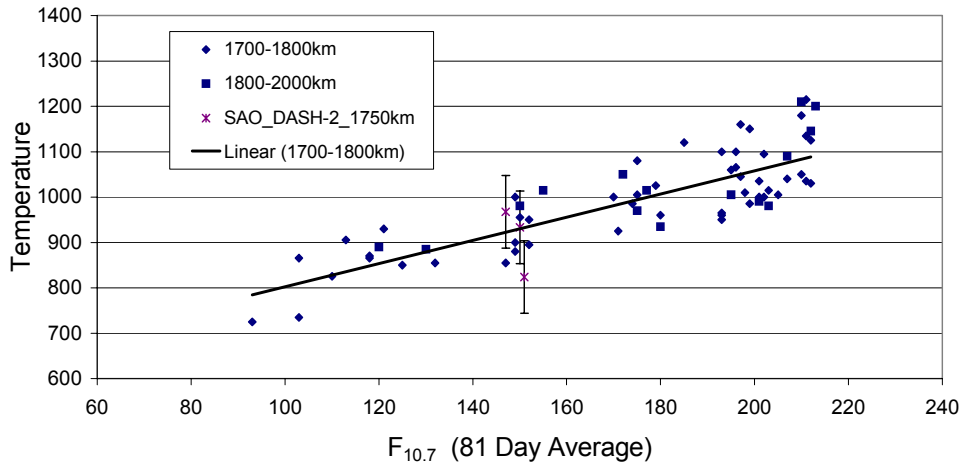


Fig. 18 He temperature for the 1700-2000 km altitude region.

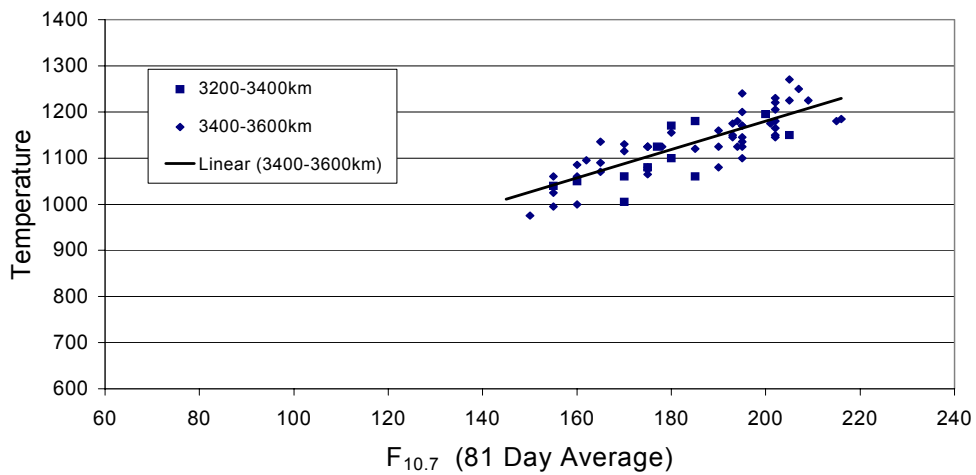


Fig. 19 He temperature for the 3200-3600 km altitude region.

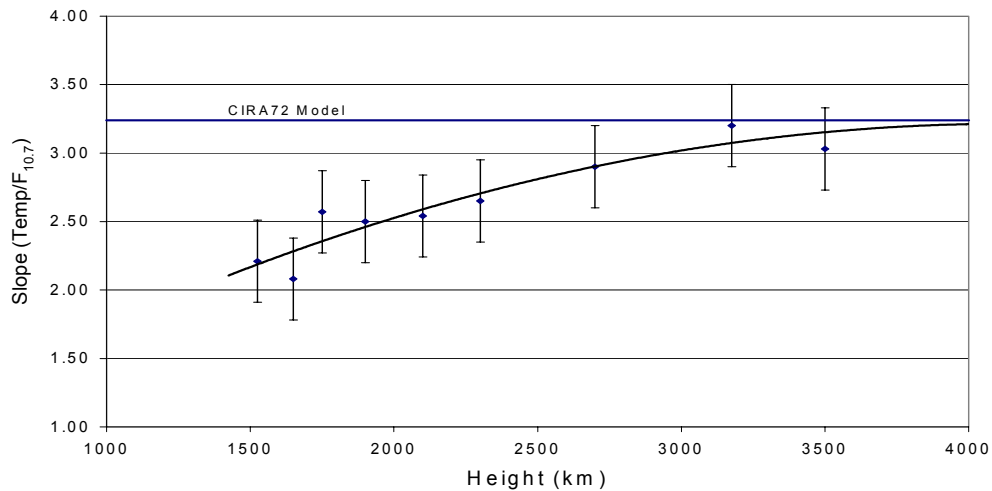


Fig. 20 He temperature slope ($\text{Temp}/\bar{F}_{10.7}$) as a function of altitude.

CONCLUSION

Density correction factors to the CIRA72 model atmosphere have been obtained from 25 satellites in the 1500 km to 4000 km altitude region. The data covered three 11-year solar cycles, which enabled density variations to be obtained as a function of the $\bar{F}_{10.7}$ solar index. The least squares fit of the density factors resulted in a new empirical model of the density variations at these altitudes as a function of height and solar activity.

REFERENCES

Afonso, G., F. Barlier, C. Berger, F. Mignard, and J. J. Walch, "Reassessment of the Charge and Neutral Drag of LAGEOS and its Geophysical Implications," *Jour. Geophys Res.*, **90**, 9381, 1985.

Anselmo, L., P. Farinella, A. Milani, and A. M. Nobili, "Effects of the Earth-reflected Sunlight on the Orbit of the LAGEOS Satellite," *Astron. and Astroph.*, **117**, 3, 1983.

Bowman, B. R., W. N. Barker, and W. G. Schick, "Orbit Perturbation Analysis of West Ford Needles Clusters," AIAA-2000-4236, *AAS/AIAA Astrodynamics Specialist Conference*, Denver, Colorado, August, 2000.

COSPAR International Reference Atmosphere 1972, Compiled by the members of COSPAR Working Group 4, Akademie-Verlag, Berlin, 1972.

Fea, K. H., and D. E. Smith, "Some Further Studies of Perturbations of Satellites at Great Altitude," *Planet. Space Sci.*, **18**, 1499, 1970.

Hedin, A. E., "A Revised Thermospheric Model Based on Mass Spectrometer and Incoherent Scatter Data: MSIS-83," *Journal Geophys. Res.*, **88**, 10170, 1983.

Hedin, A. E., "MSIS-86 Thermospheric Model," *Journal Geophys. Res.*, **92**, 4649, 1987.

Hedin, A. E., "Extension of the MSIS Thermosphere Model into the Middle and Lower Atmosphere," *Journal Geophys. Res.*, **96**, 1159, 1991.

- Jacchia, L. G., *New Static Models of the Thermosphere and Exosphere with Empirical Temperature Profiles*, Smithsonian Astrophys. Special Report 313, 1970.
- Jacchia, L. G., *Revised Static Models of the Thermosphere and Exosphere with Empirical Temperature Profiles*, Smithsonian Astrophys. Special Report 332, 1971.
- Jacchia, L. G., *Thermospheric Temperature, Density, and Composition: New Models*, Smithsonian Astrophys. Special Report 375, 1977.
- King-Hele, D., *Theory of Satellite Orbits in an Atmosphere*, Butterworths, London, 1964.
- Koskela, P. E., "Orbital Effects of Solar Radiation Pressure on an Earth Satellite," *Journal of Astronautical Sciences*, **9**, 71, 1962.
- Pardini, C., and L. Anselmo, "Calibration of Semi-Empirical Atmosphere Models Through the Orbital Decay of Spherical Satellites," *AAS/AIAA Astrodynamics Specialist Conference*, Girdwood, Alaska, August, 1999.
- Rousseau, M., "Densities Deduced from Perturbations at High Altitudes," *Planet. Space Sci.*, **21**, 1705, 1973.
- Prior, E. J., "Observed Effects of Earth-Reflected Radiation and Hydrogen Drag on the Orbital Accelerations of Balloon Satellites," *Symposium on the Use of Artificial Satellites for Geodesy*, Washington, D.C., 1971.
- Rubincam, D. P., "Drag on the Lageos Satellite," *Journal of Geophysical Research*, **95**, B4, 4881, 1990.
- Slowey, J. W., "Radiation-Pressure and Air-Drag Effects on the Orbit of the Balloon Satellite 1963 30D," Smithsonian Astrophys. Obs. Special Report 356, 1974.
- U. S. Standard Atmosphere Supplements, 1966*, ESSA, NASA, and U. S. Air Force, Dec., 1966.